
Improving Adversarial Discriminative Domain Adaptation

Aaron Chadha, Yiannis Andreopoulos

Department of Electronic and Electrical Engineering
University College London

Roberts Building, Torrington Place, London, WC1E 7JE, UK
{aaron.chadha.14,i.andreopoulos}@ucl.ac.uk

Abstract

Adversarial discriminative domain adaptation (ADDA) is an efficient framework for unsupervised domain adaptation, where the source and target domains are assumed to have the same classes, but no labels are available for the target domain. While ADDA has already achieved significant training efficiency and competitive accuracy in comparison to generative adversarial networks, we investigate whether we can allow for further improvements in its convergence properties by incorporating source label knowledge during target domain training. To achieve this, our approach first modifies the discriminator output to jointly predict the source labels *and* distinguish inputs from the target domain. We then leverage on the various source/target and encoder/discriminator distribution combinations to propose two loss functions for adversarial training of the target encoder. Our final design minimizes the maximum mean discrepancy between source encoder and target discriminator distributions, which ties together adversarial and discrepancy-based loss functions that are frequently considered independently in recent deep learning domain adaptation methods. Beyond validating our framework on standard datasets like MNIST, MNIST-M, USPS and SVHN, we introduce and evaluate on a neuromorphic vision sensing (NVS) sign language recognition dataset, where the source domain constitutes emulated neuromorphic spike events converted from APS video and the target domain is experimental spike events from an NVS camera. Our results on all datasets show that our proposal is both simple and efficient, as it competes or outperforms the state-of-the-art in unsupervised domain adaptation.

1 Introduction

The long-standing goal in visual learning is to generalize the learned knowledge from a source domain to new domains, even without the presence of labels in the target domains. Significant strides have been made towards this goal in the last few years, mainly due to proposals based on multilayered convolutional neural networks that have shown cross-domain generalizations and fast learning of new tasks by fine-tuning on limited subsets of labelled data.

Unsupervised domain adaptation directly aims at improving the generalization capability between a labelled source domain and an unlabelled target domain. Deep domain adaptation methods can generally be categorized as either being discrepancy based or adversarial based, with the common end goal of minimizing the difference between the source and target distributions. Adversarial methods in particular have become increasingly popular due to their simplicity in training and success in minimizing the domain shift. In this paper we focus on the recently proposed adversarial discriminative domain adaptation (ADDA) [1], which is related to generative adversarial learning and uses the GAN [2] objective to train on the target domain adversarially until it is aligned to the

source domain. Whilst ADDA pretrains on the source domain with labels, it throws source label information away during adversarial training. We propose to improve the convergence properties of the adversarial framework, by training the discriminator with source labels. Additionally, we leverage on the encoder and discriminator output distributions to propose both a pseudo-label and maximum mean discrepancy (MMD) [3] based loss function. We evaluate on standard domain adaptation tasks with digits datasets on which we surpass the performance of ADDA and remain competitive to other recent proposals. Finally, we introduce and validate our proposal on a new emulated-to-real neuromorphic vision sensing (NVS) dataset for sign language recognition, in which we substantially improve on accuracy compared to training on the source only.

2 Related Work

Discrepancy based methods. Discrepancy based methods typically minimize the maximum mean discrepancy (MMD) [3] loss for this purpose. For example, Tzeng *et al.* [4] proposed the deep domain confusion (DDC) method which applied a joint classification and linear MMD loss on an intermediate adaptation layer. Long *et al.* [5] extended on DDC by adding multiple task-specific adaptation layers and minimizing the domain shift with a multiple-kernel maximum mean discrepancy. Rather than matching the marginal distributions, the joint adaptation network (JAN) [6] aligns the domain shift between the joint distributions of input features and output labels. The DSN proposed by Boumalis *et al.* [7] embeds the MMD or adversarial loss as similarity losses in an overarching system of private and shared encoders. Notably, the MMD is commonly used with a Gaussian kernel, which from the Taylor expansion enables matching between all moments of distributions, albeit with some cost in processing. Alternatively, CORAL [8] matches only the mean and covariance between distributions whilst still maintaining competitive performance. More recently, Hauessuer *et al.* [9] proposed associative domain adaptation that replaces the MMD with an efficient discrepancy-based alternative that reinforces association between source and target embeddings.

Adversarial based methods. Adversarial based methods opt for an adversarial loss to minimize the domain shift. The domain adversarial neural network (DANN) [10] first introduced a gradient reversal layer that reversed the gradients of a binary classifier predicting the domain in order to train for domain confusion. Other recent proposals [11, 12, 13] have explored generative models such as GANs [2, 14] to learn from synthetic source and target data. These approaches typically train two GANs on the source and target input data with tied parameters. In order to circumvent the need to generate images, ADDA [1] was recently proposed as an adversarial framework for directly minimizing the distance between the source and target encoded representations. A discriminator and target encoder are iteratively optimized in a two-player game akin to the original GAN setting, where the goal of the discriminator is to distinguish the target representation from the source domain and the goal of target encoder is to confuse the discriminator. This implicitly aligns the target distribution to the (fixed) source distribution. The simplicity and power of ADDA has been demonstrated in visual adaptation tasks like MNIST, USPS and SVHN digits datasets. Volpi *et al.* [15] further build on ADDA by adding back in a generative component that generates augmented features for more rigorous training. Conversely, we note that ADDA throws away source label information during adversarial training. We propose to embed the source label knowledge into the discriminator and train the target encoder with a pseudo-label or discrepancy based loss, thus creating a hybrid approach for unsupervised domain adaptation.

The need for domain adaptation in NVS domain. A pertinent example of a domain where it is difficult to obtain labelled data is neuromorphic vision sensing (NVS). NVS cameras produce coordinates and timestamps of on/off spikes in an asynchronous manner, i.e., when the logarithm of the intensity value of a CMOS sensor grid position changes beyond a threshold due to scene luminance changes. While such cameras are now gaining traction as a low-power/high-speed visual sensing technology that circumvents the limitations of conventional active pixel sensing (APS) cameras, there are currently very limited or no annotations in the NVS domain for higher-level semantic tasks. This has been widely recognized to be hampering progress in the development of NVS hardware within practical applications. Emulation from APS to NVS has attempted to provide for a solution [16], and our proposals for improving ADDA training are put to the test for this challenging domain adaptation problem.

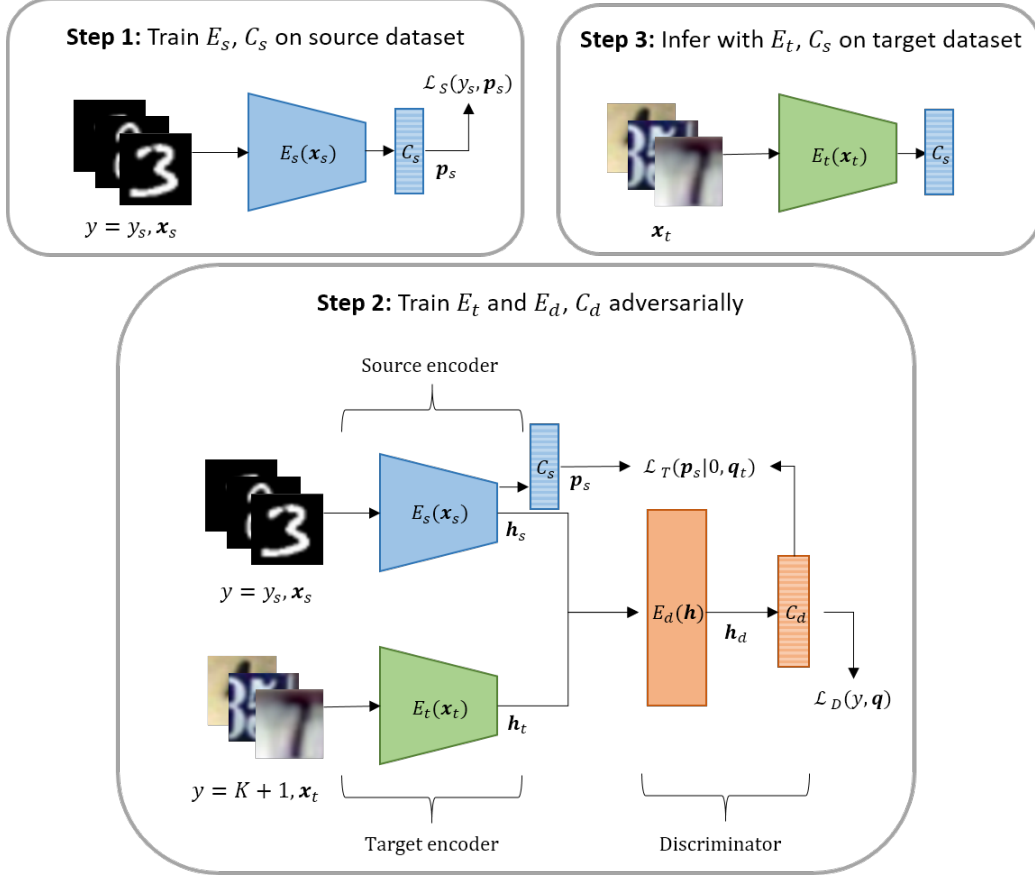


Figure 1: Improved adversarial discriminative domain adaptation. Notably, we incorporate the source labels into the adversarial training in step 2 and train the target encoder E_t by aligning the target discriminator distribution to the source encoder distribution. The figure shows the best configuration for training and inference explored in the paper.

3 Improving Adversarial Adaptation

We illustrate the framework for improving unsupervised adversarial discriminative domain adaptation in Figure 1. Let $\mathbf{X}_S = \{(\mathbf{x}_s^i, y_s^i)\}_{i=0}^{N_s}$ represent the set of source image and label pairs, where $(\mathbf{x}_s, y_s) \sim \mathbb{D}_S$ and $\mathbf{X}_T = \{(\mathbf{x}_t^i)\}_{i=0}^{N_t}$ represent the set of unlabeled target images, $\mathbf{x}_t \sim \mathbb{D}_T$. Let $E_s(\mathbf{x}_s; \theta_s)$ represent the source encoder function, parameterized by θ_s which maps an image \mathbf{x}_s to the encoder output \mathbf{h}_s , where $(\mathbf{h}_s, y_s) \sim \mathbb{P}_S$. Likewise, let $E_t(\mathbf{x}_t; \theta_t)$ represent the source encoder function, parameterized by θ_t which maps an image \mathbf{x}_t to the encoder output \mathbf{h}_t , where $\mathbf{h}_t \sim \mathbb{P}_T$. In addition, C_s represents a classifier function that maps the encoder output \mathbf{h} to class probabilities \mathbf{p} . In this paper, we only consider \mathbf{h}_s and \mathbf{h}_t as representing the source and target logits respectively and therefore C_s simply denotes the softmax function on the logits. Finally, let $E_d(\mathbf{h}; \phi_d)$ represent an encoder mapping from \mathbf{h} to an intermediate representation, and C_d represent a classifier function on said representation; E_d and C_d jointly constitute our discriminator mapping, which we refer to as $D = C_d(E_d)$. Our method is comprised of three steps, which involve learning the source mapping on the source dataset, aligning the source and target domains via adversarial training and finally inferring on the target dataset. In the proposed unsupervised framework we make the following two assumptions: first, that we have access to the source domain labels y_s during training but not the target domain labels and second, that there are no additional labels in the source or target domains. That is, the classifier C_s is fully interchangeable between the source encoder E_s and the target encoder E_t . This means we can embed C_s into the adversarial training of the target encoder E_t and discriminator D , in order to provide the discriminator with source label knowledge and increased stability during training.

3.1 Step 1: Supervised training of the source encoder and classifier

Given that we have access to labels in the source domain, we first train the source encoder E_s and classifier C_s on the source image and label pairs $(\mathbf{x}_s, y_s \in \{1, \dots, K\})$ in a supervised fashion, by minimizing the standard cross entropy loss with K classes:

$$\mathcal{L}_S = -\mathbb{E}_{(\mathbf{x}_s, y_s) \sim \mathbb{P}_S} \sum_{k=1}^K 1_{[k=y_s]} \log C_s(E_s(\mathbf{x}_s)) \quad (1)$$

The source encoder parameters ϕ_s are now frozen, which fixes the distribution \mathbb{P}_S . This becomes our reference distribution for adversarial training, analogous to the real image distribution in the GAN setting, where our aim is now to align the target distribution \mathbb{P}_T to \mathbb{P}_S by learning a suitable target encoding E_t .

3.2 Step 2: Adversarial training of the target encoder

We train the target encoder adversarially by passing the source and target encoder outputs, h_s and h_t , into a discriminator D . As per convention in an adversarial setting, the goal of the discriminator is to distinguish between the source and target domain inputs, whereas the goal of the target encoder is to fool the discriminator into confusing between the source and target domains. The target encoder and discriminator are trained alternately until the discriminator is unable to distinguish between the two domains. In doing so, we implicitly align the target encoder distribution to that of the source; i.e., $E_t(\mathbf{x}_t) \sim \mathbb{P}_S$. As the source encoder has fixed parameters, we learn an asymmetric target encoding with untied weights, which is the standard setting in both ADDA [1] and GAN implementations [2, 14]. In addition, we can improve the convergence properties by first initializing the target encoder weights with the source encoder weights; i.e., $\theta_t = \theta_s$.

We now consider how to train the target encoder and discriminator adversarially. Rather than training the discriminator and target encoder with the standard GAN loss formulations (i.e., training a logistic function on the discriminator by assigning labels 0 and 1 to the source and target domains respectively and training the generator with inverted labels [2]), we take advantage of the fact that we have access to all source labels, y_s , and show how this is additional source of information can be exploited during discriminative adversarial training. Our approach is inspired by semi-supervised GANs [17, 18], where it has been found that incorporating source label knowledge into the discriminator can jointly improve classification performance and quality of images produced by the generator. Under the discriminative adversarial framework, we can equivalently incorporate source label knowledge by replacing the discriminator logistic function with a $K + 1$ multi-class classifier, where C_d simply denotes the softmax function on the discriminator logits. As such, the discriminator output $\mathbf{q} = D(\mathbf{h})$ is a $K + 1$ dimensional vector representing the class probabilities, in which the first K dimensions represent the task-specific classes $y \in \{1, \dots, K\}$ and the final $K + 1$ dimension represents the ‘target’ class $y = K + 1$, assigned to inputs from the target domain. The discriminator is trained to jointly predict the source label y_s for source encodings \mathbf{h}_s and predict target encoding instances \mathbf{h}_t . As such our loss function for training the discriminator is now:

$$\mathcal{L}_D = -\mathbb{E}_{(\mathbf{h}_s, y_s) \sim \mathbb{P}_S} \sum_{k=1}^{K+1} 1_{[k=y_s]} \log(D(\mathbf{h}_s)) - \mathbb{E}_{(\mathbf{h}_t) \sim \mathbb{P}_T} \sum_{k=1}^{K+1} 1_{[k=K+1]} \log(D(\mathbf{h}_t)) \quad (2)$$

In order to train the target encoder adversarially, we want the target encoder to generate an output that is representative of one of the first K task-specific classes rather than the $K + 1$ -th ‘target’ class that it is assigned when training the discriminator. One option is to minimize the GAN game value, which constitutes the unsupervised component of \mathcal{L}_D . However, as in the GAN setting, this can introduce vanishing gradients due to the discriminator being too strong early in learning. We instead propose to assign a pseudo-label to the target images, which is comparable to the inverted label setting in that both are instance-based (assign a label to each instance), but draws parallels to unsupervised domain adaptation work that use pseudo-labels (typically in conjunction with co-training). The pseudo-label

is taken as the index of the maximum of the first K discriminator logits \mathbf{h}_d . In other words, denoting $\hat{y}_t = \operatorname{argmax}_{j \in 1, \dots, K} \mathbf{h}_{d,j}$:

$$\mathcal{L}_T = -\mathbb{E}_{(\mathbf{h}_t) \sim \mathbb{P}_T} \sum_{k=1}^K 1_{[k=\hat{y}_t]} \log(D(\mathbf{h}_t)) \quad (3)$$

The second option is to leverage on the two source posteriors, \mathbf{p}_s and \mathbf{q}_s , generated by the source encoder and discriminator respectively. Contrary to supervised domain adaptation methods, there are no known source and target pairwise correspondences and we cannot formulate a paired test over the posteriors. However, we can formulate the problem as a two-sample test by considering the distribution over target discriminator posteriors \mathbf{q}_t compared to the distribution over the source encoder posteriors, where our null hypothesis is that the distributions are equal. We consider a set of target posteriors $\mathbf{Q}_T = \{\mathbf{q}_t^1, \dots, \mathbf{q}_t^m\} \sim \mathbb{Q}$ and a set of source posteriors $\mathbf{P}_S = \{\mathbf{p}_s^1, \dots, \mathbf{p}_s^n\} \sim \mathbb{P}$. Effectively, we want to minimize the distance between \mathbb{P} and \mathbb{Q} without performing any density estimation. To this end, we adopt the Maximum Mean Discrepancy (MMD) [3] metric as a measure of distance between the mean embeddings of \mathbf{p}_s and \mathbf{q}_t . For reproducing kernel Hilbert space (RKHS) \mathcal{H} , function class $\mathcal{F} = \{f : \|f\| \leq 1\}$ and infinite dimensional feature map $\phi : \mathcal{X} \rightarrow \mathcal{H}$ the MMD can be expressed as:

$$\mathcal{D}_{\text{MMD}} = \sup_{f \in \mathcal{F}, \|f\|_{\mathcal{H}} \leq 1} |\mathbb{E}_{\mathbf{p}_s \sim \mathbb{P}} f(\mathbf{p}_s|0) - \mathbb{E}_{\mathbf{q}_t \sim \mathbb{Q}} f(\mathbf{q}_t)| = \|\mathbb{E}_{\mathbf{p}_s \sim \mathbb{P}} \phi(\mathbf{p}_s|0) - \mathbb{E}_{\mathbf{q}_t \sim \mathbb{Q}} \phi(\mathbf{q}_t)\|_{\mathcal{H}} \quad (4)$$

We note that MMD employed in our proposal can be interpreted as matching all moments between the source and target distributions, whereas conventional feature matching (as in [18]) is only empirically matching the first order moments (means) of the intermediate discriminator layer activations. Specifically, we are performing distribution alignment of the target encoder posteriors (i.e., post-softmax) to the source encoder posteriors extended over $K + 1$ classes, in order to train the target encoder adversarially. Importantly, the distribution over source encoder posteriors does not change during adversarial training as the source encoder is fixed. We append a 0 to the source encoder posteriors to represent the target class probability, such that both source and target posteriors are $K + 1$ dimensional prior to mapping to \mathcal{H} . This zero constraint on the target class acts as a stronger prior upon which to learn the target encoder; as such, the source encoder posterior provides a more informative representation than the source discriminator posterior.

The feature map ϕ in equation 4 corresponds to a PSD kernel k such that $k(\mathbf{x}, \mathbf{y}) = \langle \phi(\mathbf{x}), \phi(\mathbf{y}) \rangle_{\mathcal{H}}$, which means we can rewrite (4) in terms of k . The loss function on our target encoder that we wish to minimize can thus be written as:

$$\mathcal{L}_T = \mathcal{D}_{\text{MMD}}^2 = \mathbb{E}_{\mathbf{p}_s, \mathbf{p}'_s \sim \mathbb{P}} k(\mathbf{p}_s|0, \mathbf{p}'_s|0) - \mathbb{E}_{\mathbf{p}_s, \mathbf{q}_t \sim \mathbb{P}, \mathbb{Q}} k(\mathbf{p}_s|0, \mathbf{q}_t) + \mathbb{E}_{\mathbf{q}_t, \mathbf{q}'_t \sim \mathbb{Q}} k(\mathbf{q}_t, \mathbf{q}'_t) \quad (5)$$

In this paper we opt to use a linear combination of r multiple RBF kernels over a range of standard deviations, such that $k(\mathbf{x}, \mathbf{y}) = \sum_r \exp\{-\frac{1}{2\sigma_r} \|\mathbf{x} - \mathbf{y}\|^2\}$, where σ_r is the standard deviation of the r -th RBF kernel. By introducing a linear combination over varying bandwidths, we improve the generalization performance over different sample distributions. This method of generalization with fixed kernels is commonly used both in generative models [19, 20] and other domain adaptation discrepancy based methods [7, 5]. To ensure consistency, we fix the kernel combination for all experiments. Specifically, after experimentation, we found that optimal performance for our framework is achieved with a summation over five kernels, with $\sigma_r = 10^{-r}$, $r \in \{0, \dots, 4\}$. Finally, we note that, in order to improve the generalization in the context of GANs, recent work [21, 22] has looked at kernel optimization by adversarially training the kernel with the discriminator or critic, such that the kernel is maximally discriminative. While, we can also perform this kernel optimization in the discriminative adversarial setting with multiple classes, we leave this for future work.

In order to substantiate the importance of our proposed MMD loss formulation, Table 1 presents results for all source/target encoder/discriminator posterior combinations and feature matching on an intermediate discriminator layer [18]. Evidently, our proposed loss formulation is key to adversarial training – it is not sufficient to just convert the discriminator from binary to multi-class and train with feature matching/standard GAN game value.

	SVHN \rightarrow MNIST	MNIST \rightarrow USPS
Source enc. \rightarrow Target disc. (our proposal)	0.885	0.884
Source disc. \rightarrow Target disc.	0.800	0.878
Source enc. \rightarrow Target enc.	0.680	0.773
Source disc. \rightarrow Target enc.	0.620	0.758
Feature matching [18]	0.682	0.799

Table 1: Accuracy on standard datasets for all considered posterior combinations + feature matching [18].

3.3 Step 3: Inference on the target dataset

After training the target encoder, we can now perform inference on the target dataset. However, we have effectively trained two sets of target predictions; namely, the mapped target encoder output $C_s(\mathbf{h}_t)$ and the discriminator output \mathbf{q}_t . In the optimal setting, where we have trained the discriminator to equilibrium, we would expect the discriminator mapped source and target distributions would be aligned—and more so with the MMD loss function where $\mathbf{q}_t \sim \mathbb{P}$, $C_s(\mathbf{h}_t) \sim \mathbb{P}$. However, we empirically find that evaluation on \mathbf{q}_t is marginally worse ($\sim 1\%$) than evaluation on $C_s(\mathbf{h}_t)$. Therefore, for the remainder of the paper, we infer on the target encoder output.

4 Experimental Results

We present experimental results on unsupervised domain adaptation task, with both target encoder loss functions. In order to compare with the recently proposed ADDA, we experiment on four digits datasets of varying sizes and difficulty: MNIST-M [10], MNIST [23], USPS and SVHN [24]. We demonstrate substantial gain over ADDA and other recent methods, which is evident on the more difficult domain adaptation tasks such as SVHN \rightarrow MNIST. In addition, since neuromorphic vision sensing presents a pertinent application for domain adaptation, we additionally introduce and validate on a new NVS sign language dataset, demonstrating substantial gain in target accuracy compared to training with the source domain only (which comprises emulated NVS data from an open-source NVS emulation framework [16]).

4.1 Digits datasets

We consider four standard domain adaptation scenarios between dataset pairs drawn from MNIST-M [10], MNIST [23], USPS and SVHN [24] digits datasets, which are each comprised of $K = 10$ digit classes (0-9). Specifically, we evaluate on MNIST \rightarrow USPS, USPS \rightarrow MNIST, SVHN \rightarrow MNIST and MNIST \rightarrow MNIST-M. The difficulty in domain adaptation task increases as the variability between datasets increases. We follow a similar training procedure of Tzeng *et al.* [1]. For the MNIST \rightarrow USPS and USPS \rightarrow MNIST experiments, we sample 2000 images from MNIST and 1800 from USPS, otherwise we train and infer on the full datasets. For MNIST \rightarrow MNIST-M, we generate the unlabelled MNIST-M target dataset by following the process described by Ganin *et al.* [10]. For all experiments we use a modified LeNet architecture [23] for the source and target encoder. The discriminator is comprised of 2 fully connected layers with 500 hidden units and a final fully-connected layer with $K + 1 = 11$ hidden units that outputs the logits. With this setup, our network is roughly the same complexity as ADDA in terms of number of parameters. In step 1, the source encoder is trained with the Adam [25] optimizer for 10k iterations with a batch size of 128 and learning rate of 0.001. In step 2, the target encoder is trained with a batch size of 128 per domain for 10k iterations but with a lower learning rate of 0.0002, $\beta_1 = 0.5$ and $\beta_2 = 0.999$. We resize all images to a fixed size of 28×28 prior to CNN processing. We additionally use data augmentation for MNIST \rightarrow MNIST-M by randomly inverting the MNIST grayscale values and replicating the MNIST inputs channel-wise to match MNIST-M dimensions. Our results are provided in Table 2 compared to the current state-of-the-art and when training on source only. We focus our comparison on ADDA [1] and DIFA [15], which are both recently proposed adversarial methods.

On the SVHN \rightarrow MNIST task, we improve on ADDA by over 10% when optimizing with either target encoder loss function. In order to isolate the performance gain from domain adaptation, we

Method	SVHN \rightarrow MNIST	USPS \rightarrow MNIST	MNIST \rightarrow USPS	MNIST \rightarrow MNIST-M
Source only	0.667	0.586	0.756	0.714
DANN [10]	0.739	0.730	0.771	0.529
DDC [4]	0.681	0.665	0.791	-
DSN [7]	0.827	-	-	0.832
DTN [13]	0.844*	-	-	-
UNIT [26]	0.905*	-	-	-
CoGAN [11]	no convergence	0.891	0.912	-
ADDA [1]	0.760 (26%)	0.901 (58%)	0.894 (19%)	0.805**(13%)
DIFA [15]	0.897 (32%)	0.897 (43%)	0.923 (28%)	-
Proposed, ADDA-MAX (3)	0.899 (35%)	0.855 (46%)	0.882 (17%)	0.800 (12%)
Proposed, ADDA-MMD (5)	0.885 (33%)	0.941 (61%)	0.884 (17%)	0.879 (23%)

Table 2: Accuracy for our proposed method with both variants of the target encoder loss function compared to the current state-of-the-art. In order to isolate the performance gain from domain adaptation for our proposals, we report in parentheses the percentage increase (relative) over the source-only accuracy, as reported in the respective papers for DIFA [11] and ADDA [1]. *UNIT [26] and DTN [13] use additional SVHN data (131 images and 531 images respectively). **This is our implementation of ADDA [1] on MNIST \rightarrow MNIST-M, as this task is not used in the original paper.

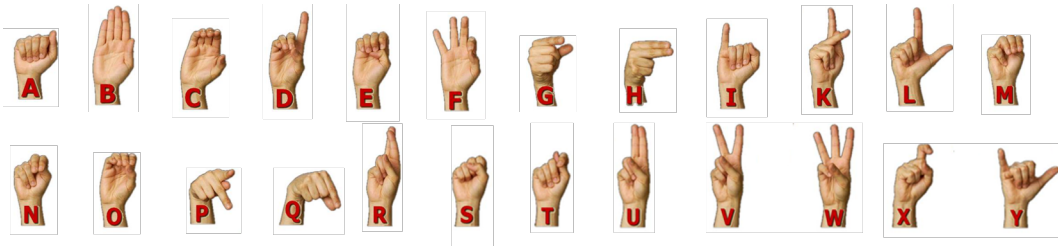


Figure 2: Signs for letters A-Z from the American Sign Language dataset. Note that some letters such as M and N only have subtle differences. Letters J and Z are excluded given that they are not static signs and require a particular gesture.

compute the percentage increase (relative) over the source only accuracy reported in the paper (shown in parentheses in Table 2). On three of the four tasks our proposed ADDA-MMD outperforms both ADDA and DIFA, in terms of absolute accuracy and/or increase over the source only accuracy. We note that ADDA and DIFA compete with our proposal on the USPS \rightarrow MNIST and MNIST \rightarrow USPS tasks, which we attribute to the size of the subsets employed for training, compared to the substantially larger MNIST and SVHN datasets. It is worth noting that the performance of ADDA-MAX is less stable than ADDA-MMD, as the loss function on the target encoder is instance based as in the original GAN setting.

4.2 NVS ASL dataset

We introduce a new sign language recognition dataset for NVS-based unsupervised domain adaptation. The primary motivation behind creating the dataset and validating our framework with it is that progress in neuromorphic spike-based event or action recognition is severely hampered from the lack of NVS training data with reliable annotations [27]. This is partially addressed via emulators like PIX2NVS [16] that convert annotated APS video datasets into emulated NVS data in order to train advanced discriminative models in a supervised manner. However, beyond the unavoidable gap between the experimental and the emulated NVS data distributions, the NVS camera technology is in constant evolution and new versions of hardware devices like DAVIS and ATIS [28] and their multiple settings cause further domain shift against their previous versions and previously-released software emulation frameworks.

Our experimental dataset is comprised of 1200 unlabelled real recordings and 1200 labelled emulated recordings, each representing a different static sign of 24 letters (A-Y, excluding J) from the America Sign Language (ASL). We note that similar to other APS-based sign language recognition tasks [29], letters J and Z are excluded as their ASL designation requires motion. Figure 2 shows the required

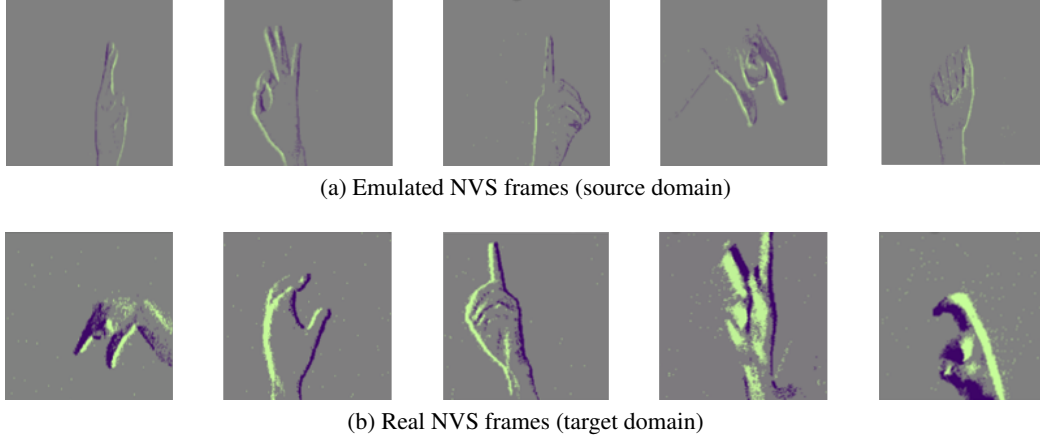


Figure 3: Select frames from the NVS American Sign Language recognition dataset. The source domain constitutes emulated NVS frames which are generated from APS recorded video with PIX2NVS [16]. The target domain constitutes real NVS frames as recorded by an iniLabs DAVIS240c NVS camera. The green/purple points correspond to the +1/-1 (or ON/OFF) spike polarity. Best viewed in color.

hand pose for each letter of the dataset. As is evident from the figure, sign language recognition presents a substantially more difficult task than digit recognition, considering that for some letters (e.g., M and N) there is very little variation in fingers’ positioning.

In order to generate the emulated spike events we first record APS video of someone performing the sign for each letter with translational and rotational motion over the video duration, thus increase the difficulty of the recognition task. Next, the APS video is recorded with a standard laptop camera, and consecutive APS frames are passed into the recently proposed PIX2NVS emulator [16], with the emulator tuned to the optimal settings. The PIX2NVS converts the APS frames to the corresponding emulated NVS frames, and this constitutes our source domain. The real NVS recordings are recorded directly with an iniLabs DAVIS240c NVS camera, again with rotational and translational motion over the video duration.

Figure 3 shows a selection of (a) emulated and (b) real NVS frames from the dataset. There is a discernible domain shift between the emulated and real spike events, with the real NVS events exhibiting a substantially higher spike density that increases the visibility of the signed letter, despite also carrying some background ‘salt & pepper’ noise. Nonetheless, we are able to demonstrate that our proposed method can reduce this domain shift. As the recordings represent static signs we train on individual frames and remove a subset of frames from the start and end of the recording where there may be no sign distinguishable. As such, we have ~80,000 emulated NVS frames for and ~55,000 real NVS frames for domain adaptation and inference. The frame resolution in both domains is 240×180 . Our source encoder is VGG16 [30], which we train in step 1 on the emulated NVS frames using stochastic gradient descent with momentum set to 0.9. The learning rate is set to 0.001, the batch size to 24 and we complete training at 15k iterations. In order to combat overfitting, we set dropout on the first two fully connected layers to 0.8. In terms of data augmentation, we first resize the input such that the smaller side is 256 and keep the aspect ratio. We then use a multi-scale random cropping of the resized RGB frame; the cropped volume is subsequently randomly flipped, and normalized according to its mean. In step 2, we follow the same procedure with dropout in the target fully connected layers and data augmentation on both input domains to train the target encoder adversarially for 10k iterations. We infer on the target dataset by extracting a single center crop.

We present both the overall and per-letter recognition accuracy in Table 3 when evaluating on the NVS ASL dataset. For clarity, we only include letters in the table with subtle differences such as M and N. We include results on our proposed framework, with both variants of target encoder loss function, along with results when evaluating with the source only. In both cases our proposal provides substantial increase in accuracy compared to training on the source only; in particular, training with the MMD loss function increases the overall accuracy by 33% and achieves over 99% accuracy on four of the letters listed. Interestingly, the letters where our proposed framework underperforms

Letter	A	B	E	F	M	N	S	T	U	V	overall
Source only	0.925	0.745	0.809	0.163	0.164	0.376	0.837	0.162	0.277	0.992	0.638
Proposed, ADDA-MMD	0.988	0.990	0.992	0.994	0.467	0.001	0.807	0.001	0.968	0.999	0.849

Table 3: Overall and per-letter recognition accuracy for select letters of the NVS ASL dataset. We evaluate on the source-only and our proposed ADDA-MMD.

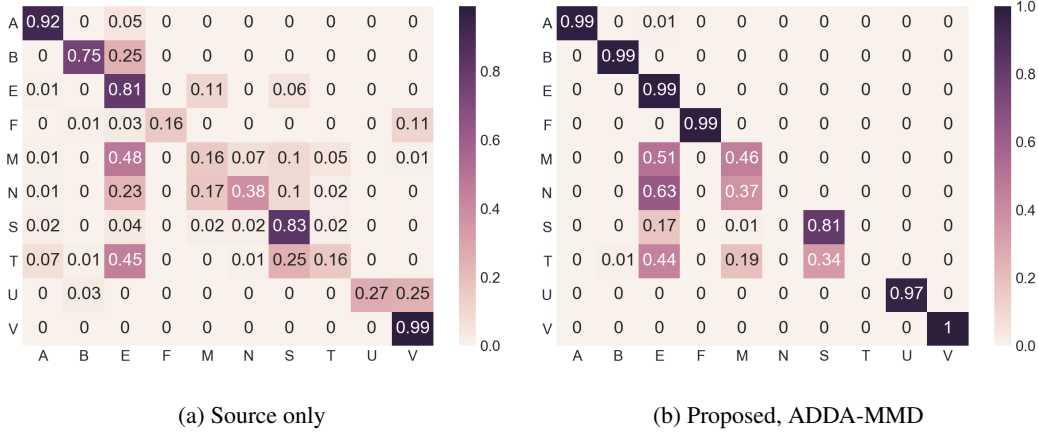


Figure 4: Confusion matrices for a) source-only and b) proposed, ADDA-MMD on select letters for sign language recognition on NVS ASL dataset. The vertical axis represents the true label and horizontal axis represents the predicted label.

compared to training on the source only are typically members of image sets that can easily be confused; one such set is $\mathbf{C} = \{E, M, N, S, T\}$. In particular, N and T experience a substantial decrease in accuracy when compared to the source only. It appears that the domain adaptation forgoes these two classes in order to learn a more aligned target distribution. If we cross-reference Table 3 with the confusion matrices plotted in Figure 4, we see that whilst the accuracy for other letters substantially increases, M,N,S,T are more commonly confused with the letter E. Note that we also attempted to train on ADDA [1] under the same settings but it consistently leads to a degenerate solution, favoring one or two classes above all others. This may be attributed to the small training batch size.

5 Conclusion

We extend adversarial discriminative domain adaptation by explicitly taking into account the source labels during target domain training. Our framework is shown to compete or outperform the state-of-the-art in unsupervised transfer learning on standard datasets, while remaining simple and intuitive to use and extend further by embedding kernel optimization into the adversarial framework. We have also performed some preliminary experiments on the standard Office-31 dataset in the fully transductive setting, and using our proposed ADDA-MMD, VGG-16 and fine-tuning only the fully-connected layers. On the hardest shift, Amazon \rightarrow Webcam, we achieve 81.6%; 7% accuracy gain over ADDA and 15% gain over source-only, which further validates our proposal. To show the efficacy of our approach for applications going beyond the standard benchmarks, we introduce a neuromorphic vision sensing dataset and show that our proposal allows for unsupervised domain adaptation between emulated and real neuromorphic spike events for a sign language recognition application.

References

- [1] Eric Tzeng, Judy Hoffman, Kate Saenko, and Trevor Darrell. Adversarial discriminative domain adaptation. In *Computer Vision and Pattern Recognition (CVPR)*, volume 1, page 4, 2017.
- [2] Ian Goodfellow, Jean Pouget-Abadie, Mehdi Mirza, Bing Xu, David Warde-Farley, Sherjil Ozair, Aaron Courville, and Yoshua Bengio. Generative adversarial nets. In *Advances in neural information processing systems*, pages 2672–2680, 2014.
- [3] Arthur Gretton, Karsten M Borgwardt, Malte J Rasch, Bernhard Schölkopf, and Alexander Smola. A kernel two-sample test. *Journal of Machine Learning Research*, 13(Mar):723–773, 2012.
- [4] Eric Tzeng, Judy Hoffman, Ning Zhang, Kate Saenko, and Trevor Darrell. Deep domain confusion: Maximizing for domain invariance. *arXiv preprint arXiv:1412.3474*, 2014.
- [5] Mingsheng Long, Yue Cao, Jianmin Wang, and Michael I Jordan. Learning transferable features with deep adaptation networks. *arXiv preprint arXiv:1502.02791*, 2015.
- [6] Mingsheng Long, Han Zhu, Jianmin Wang, and Michael I Jordan. Deep transfer learning with joint adaptation networks. *arXiv preprint arXiv:1605.06636*, 2016.
- [7] Konstantinos Bousmalis, George Trigeorgis, Nathan Silberman, Dilip Krishnan, and Dumitru Erhan. Domain separation networks. In *Advances in Neural Information Processing Systems*, pages 343–351, 2016.
- [8] Baochen Sun and Kate Saenko. Deep coral: Correlation alignment for deep domain adaptation. In *European Conference on Computer Vision*, pages 443–450. Springer, 2016.
- [9] Philip Haeusser, Thomas Frerix, Alexander Mordvintsev, and Daniel Cremers. Associative domain adaptation. In *International Conference on Computer Vision (ICCV)*, volume 2, page 6, 2017.
- [10] Yaroslav Ganin, Evgeniya Ustinova, Hana Ajakan, Pascal Germain, Hugo Larochelle, François Laviolette, Mario Marchand, and Victor Lempitsky. Domain-adversarial training of neural networks. *The Journal of Machine Learning Research*, 17(1):2096–2030, 2016.
- [11] Ming-Yu Liu and Oncel Tuzel. Coupled generative adversarial networks. In *Advances in neural information processing systems*, pages 469–477, 2016.
- [12] Konstantinos Bousmalis, Nathan Silberman, David Dohan, Dumitru Erhan, and Dilip Krishnan. Unsupervised pixel-level domain adaptation with generative adversarial networks. In *The IEEE Conference on Computer Vision and Pattern Recognition (CVPR)*, volume 1, page 7, 2017.
- [13] Yaniv Taigman, Adam Polyak, and Lior Wolf. Unsupervised cross-domain image generation. *arXiv preprint arXiv:1611.02200*, 2016.
- [14] Mehdi Mirza and Simon Osindero. Conditional generative adversarial nets. *arXiv preprint arXiv:1411.1784*, 2014.
- [15] Riccardo Volpi, Pietro Morerio, Silvio Savarese, and Vittorio Murino. Adversarial feature augmentation for unsupervised domain adaptation. *arXiv preprint arXiv:1711.08561*, 2017.
- [16] Yin Bi and Yiannis Andreopoulos. Pix2nvs: Parameterized conversion of pixel-domain video frames to neuromorphic vision streams. In *Image Processing (ICIP), 2017 IEEE International Conference on*, pages 1990–1994. IEEE, 2017.
- [17] Augustus Odena. Semi-supervised learning with generative adversarial networks. *arXiv preprint arXiv:1606.01583*, 2016.
- [18] Tim Salimans, Ian Goodfellow, Wojciech Zaremba, Vicki Cheung, Alec Radford, and Xi Chen. Improved techniques for training gans. In *Advances in Neural Information Processing Systems*, pages 2234–2242, 2016.

- [19] Yujia Li, Kevin Swersky, and Rich Zemel. Generative moment matching networks. In *International Conference on Machine Learning*, pages 1718–1727, 2015.
- [20] Gintare Karolina Dziugaite, Daniel M Roy, and Zoubin Ghahramani. Training generative neural networks via maximum mean discrepancy optimization. *arXiv preprint arXiv:1505.03906*, 2015.
- [21] Chun-Liang Li, Wei-Cheng Chang, Yu Cheng, Yiming Yang, and Barnabás Póczos. Mmd gan: Towards deeper understanding of moment matching network. In *Advances in Neural Information Processing Systems*, pages 2200–2210, 2017.
- [22] Youssef Mroueh, Tom Sercu, and Vaibhava Goel. Mcgan: Mean and covariance feature matching gan. *arXiv preprint arXiv:1702.08398*, 2017.
- [23] Yann LeCun, Léon Bottou, Yoshua Bengio, and Patrick Haffner. Gradient-based learning applied to document recognition. *Proceedings of the IEEE*, 86(11):2278–2324, 1998.
- [24] Yuval Netzer, Tao Wang, Adam Coates, Alessandro Bissacco, Bo Wu, and Andrew Y Ng. Reading digits in natural images with unsupervised feature learning. In *NIPS workshop on deep learning and unsupervised feature learning*, volume 2011, page 5, 2011.
- [25] Diederik P Kingma and Jimmy Ba. Adam: A method for stochastic optimization. *arXiv preprint arXiv:1412.6980*, 2014.
- [26] Ming-Yu Liu, Thomas Breuel, and Jan Kautz. Unsupervised image-to-image translation networks. In *Advances in Neural Information Processing Systems*, pages 700–708, 2017.
- [27] Cheston Tan, Stephane Lallee, and Garrick Orchard. Benchmarking neuromorphic vision: lessons learnt from computer vision. *Frontiers in neuroscience*, 9:374, 2015.
- [28] Tobi Delbruck. Neuromorphic vision sensing and processing. In *Solid-State Device Research Conference (ESSDERC), 2016 46th European*, pages 7–14. IEEE, 2016.
- [29] Nicolas Pugeault and Richard Bowden. Spelling it out: Real-time asl fingerspelling recognition. In *Computer Vision Workshops (ICCV Workshops), 2011 IEEE International Conference on*, pages 1114–1119. IEEE, 2011.
- [30] Karen Simonyan and Andrew Zisserman. Very deep convolutional networks for large-scale image recognition. *arXiv preprint arXiv:1409.1556*, 2014.